pubs.acs.org/Biomac

Article

Protein Extraction Efficiency and Selectivity of Esterified Styrene–Maleic Acid Copolymers in Thylakoid Membranes

Nathan G. Brady,[‖] Cameron E. Workman,[‖] Bridgie Cawthon, Barry D. Bruce,* and Brian K. Long*

Cite This: *Biomacromolecules* 2021, 22, 2544–2553

Read Online

ACCESS | Metrics & More | Article Recommendations | Supporting Information

ABSTRACT: Amphiphilic styrene–maleic acid copolymers (SMAs) have been shown to effectively extract membrane proteins surrounded by an annulus of native membrane lipids via the formation of nanodiscs. Recent reports have shown that 2-butoxyethanol-functionalized SMA derivatives promote the extraction of membrane proteins from thylakoid membranes, whereas unfunctionalized SMA is essentially ineffective. However, it is unknown how the extent of functionalization and identity of sidechains impact protein solubilization and specificity. Herein, we show that the monoesterification of an SMA polymer with hydrophobic alkoxy ethoxylate sidechains leads to an increased solubilization efficiency (SE) of trimeric photosystem I (PSI) from the membranes of cyanobacterium *Thermosynechococcus elongatus*. The specific SMA polymer used in this study, PRO 10235, cannot encapsulate single PSI trimers from this cyanobacterium; however, as it is functionalized with alkoxy ethoxylates of increasing alkoxy chain length, a clear increase in the trimeric PSI SE is observed. Furthermore, an exponential increase in the SE is observed when >50% of the maleic acid repeat units are monoesterified with long alkoxy ethoxylates, suggesting that the PSI extraction mechanism is highly dependent on both the number and length of the attached side chains.

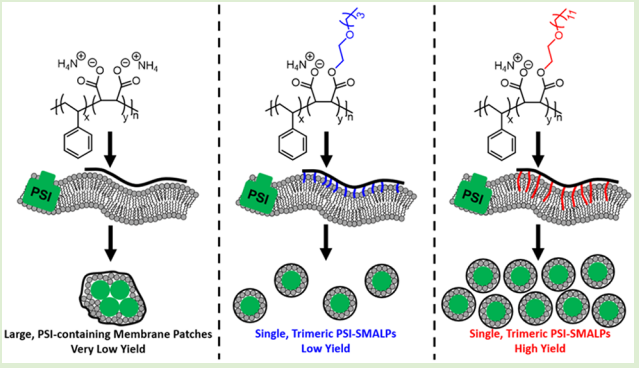

INTRODUCTION

Over the past decade, styrene–maleic acid copolymers (SMAs) have become widely used for the solubilization of membrane proteins. Their unique ability to form styrene–maleic acid lipid particles (SMALPs), which are polymer bound nanodiscs composed of proteins within an annulus of retained native lipids, has made these amphiphilic copolymers the subject of numerous investigations.[1] Salient reports include studies designed to understand how various SMA molecular characteristics play into the SMALP formation and efficacy of these polymers in protein extraction. For example, it has been shown that both the molecular weight of the polymer[2] and the incorporation ratio of the monomeric units[3] are both crucial parameters in this process.

Despite these advances, little is known about the mechanism of SMA-facilitated protein extraction and solubilization. Many studies designed to probe this mechanism have shown that altering the chemical composition of SMA can result in characteristic changes in nanodisc formation. Examples of such investigations include studies by Ramamoorthy and co-workers in which the maleic anhydride repeating units of SMA copolymers were converted into maleimides bearing quaternary ammonium pendant groups, increasing the polymer's tolerance to divalent cations and low pH.[4] In another study, Konkolewicz and Lorigan achieved a similar result by performing esterification and amidation reactions on SMAs using a variety of moieties, ranging from glucose to 2-aminoethanol.[5] Overduin and co-workers showed that SMA functionalization can be used to manipulate the size of resulting SMALPs, further highlighting how functionalized SMA samples can be utilized to alter various aspects of the protein extraction process.[6] Although all of these studies demonstrate the effects of SMA functionalization, they did not investigate how SMA functionalization alters the extraction efficiency or selectivity in specific protein solubilization trials. An understanding of the fundamental relationships between specific SMA derivatization and the resultant extraction selectivity and/or efficiency could facilitate the selection and design of SMAs with enhanced extraction yields, as well as the potential to target specific proteins.

Bruce and co-workers have recently shown that certain commercially available SMA-based copolymers exhibit the ability to form SMALPs from chloroplast thylakoid membranes,[7] which is of note because of the lack of studies

Received: March 3, 2021
Revised: May 12, 2021
Published: May 26, 2021

investigating galactolipid-rich membranes. Furthermore, their investigations in cyanobacterial thylakoid membranes showed that commercially available SMA 1440 (Total Cray Valley), a 1.5:1 styrene:maleic acid copolymer that is 72% monoesterified with butoxyethanol, appears to selectively extract photosystem I (PSI) trimer from the thylakoid membranes of *Thermosynechococcus elongatus* (Te), whereas the most widely used SMA copolymers, those containing a 2:1 ratio of styrene:maleic acid, are ineffective.[8] This is of interest as the nonesterified version of the same SMA, PRO 10235, shows very little activity in the extraction of PSI from thylakoid membranes in Te.[9] In addition, PRO 10235 demonstrated the lowest extraction activity among the five tested SMAs using thylakoids from pea and spinach chloroplasts,[7] suggesting a generally lower activity with galactolipid-rich membranes. We hypothesized that the butoxyethanol esterification of SMA 1440 must be critical for polymer insertion into the galactolipid-rich thylakoid membranes of cyanobacteria. To probe this possibility, we herein present a series of derivatized SMA copolymers that are functionalized to various extents with alkoxy ethoxylates of increasing chain lengths to test the impact that alkyl sidechains have on the protein extraction efficiency and selectivity from Te.

EXPERIMENTAL SECTION

General Materials and Methods. All chemical reagents were obtained from commercial sources and used without further purification, unless otherwise noted. 2-Octyloxyethanol, 2-decyloxyethanol, and 2-dodecyloxyethanol were synthesized using a modified literature procedure.[10] PRO 10235 was obtained from Cray Valley (now Polyscope). One important note is that the specific batch of PRO 10235 used in this study was experimentally found to have a 1.21:1 ratio of styrene:maleic anhydride by ^{1}H NMR spectroscopy (Figure S1). Tetrahydrofuran (THF) was dried using an Innovative Technology Pure Solv solvent purification system. Water was purified using a MilliQ Biocel reverse osmosis system with a resistance of >18 MΩ to mitigate the impact of trace ions. ^{1}H NMR spectroscopy was performed using a Varian 500 MHz NMR spectrometer, and chemical shifts are reported with respect to residual solvent peaks.

General Synthesis of Alkoxy Ethoxylates. In a typical procedure, a mixture of KOH (9.26 g, 165 mmol) in ethylene glycol (42 mL, 750 mmol) was added to 1,4-dioxane (90 mL), Bu_4NBr (2.9 g, 9 mmol), and 1-bromoalkane (150 mmol). The reaction mixture was then heated to 105 °C for 5 h. The mixture was cooled to room temperature and extracted with $CHCl_3$ (×3). The organic layer was separated, washed with water (×3), concentrated under vacuum, and the remaining residue purified via vacuum distillation to provide each product as a clear oil. Yields for 2-octyloxyethanol, 2-decyloxyethanol, and 2-dodecyloxyethanol were 60, 64, and 73%, respectively. The characterization of each product agreed with prior literature reports.[10]

Esterification of PRO 10235. Esterification was performed using a modified literature procedure.[11] PRO 10235 (2.5 g, 9.8 mmol) was dissolved in dry THF (45 mL), followed by the addition of a 4-dimethylaminopyridine (DMAP) (0.06 g, 0.05 mmol) solution in dry THF (5 mL). The target alcohol (80 mmol) was then added to the polymer solution. The reaction was stirred under constant reflux for prescribed time intervals. Therein, ∼8 mL aliquots were taken at various time points in order to achieve varying extents of esterification. To each aliquot was added HCl solution (10 mL, 0.001 M). The organic layer was decanted, concentrated under vacuum, and dried in a vacuum oven at 80 °C for a minimum of 24 h.

Determination of the Esterification Percentage. Utilizing the experimentally determined incorporation ratio of 1.21:1 styrene:maleic anhydride in PRO 10235, the extent of esterification was determined via ^{1}H NMR spectroscopy by comparing the integration of the aryl region to the proton signal corresponding to the methyl protons of the attached sidechain (Figure S2). All NMR spectra for modified SMAs can be seen in Figures S3-S11. Diffusion-ordered spectroscopy nuclear magnetic resonance (DOSY NMR) was also used to confirm the functionalization of the polymer backbone with the desired alcohol rather than free alcohol remaining in the solution (Figure S12).

Solubilization of the Prepared SMA Derivatives. The solubilization of the SMA derivatives was performed by placing the target SMA (15% w/v) in water (80% w/v) and adding a solution of 30% NH_4OH in water (5% w/v). Each solution was heated at 80 °C for ≥30 min until a nonturbid solution was obtained.

Determination of pH and Divalent Cations Sensitivity in Aqueous Media. The solubility of each polymer sample as a function of pH was determined using a modified literature procedure.[12] Therein, each polymer sample was diluted into a standard Britton−Robinson (BR)[12] buffer containing 150 mM NaCl for a final concentration of 0.15% (w/v). The prepared buffers ranged from pH 4.5 to 10 in half unit increments. The samples were then mixed via orbital shaking for 10 min, and the optical density was measured at 350 nm using an ultraviolet (UV) spectrometer. Optical density values above the baseline were interpreted as an indicator of polymer aggregation and precipitation from the solution.

Divalent cation sensitivity was also determined using a modified literature procedure.[5] Each polymer sample was diluted into a 9.5 pH tris buffer containing various concentrations of $MgCl_2$, ranging from 1 to 100 mM. The final concentration of each polymer solution was 0.15% (w/v). These solutions were then mixed via orbital shaking for 10 min, and the optical density was measured at 350 nm using a UV spectrometer. The optical density values above the baseline were interpreted as an indicator of polymer aggregation and precipitation from the solution.

Critical Aggregation Concentration Determination. The critical aggregation concentration (CAC) for the tested polymer samples was determined following a previous literature procedure.[12] Therein, each polymer sample was diluted to 0.15% (w/v) in a standard BR-buffer at a pH of 9.5. These polymer solutions were placed into a 96-well plate, and each sample was diluted fivefold (×12) across the wells. A Nile Red solution was added to each well at a concentration of 1 μM. Each plate was excited at 550 nm, and the emission was measured between 550−700 nm in 1 nm increments. The wavelength of the highest emission intensity was plotted versus concentration for each polymer sample. The CAC was determined by fitting sigmoidal curves to the blue-shifting fluorescence spectra as the polymer concentration increased.

Preparation of Thylakoid Membranes. Thylakoid membranes were isolated following established protocols.[8] Briefly, Te cells were grown in BG-11 media, in an air lift, flat panel bioreactor at 45 °C (Photon Systems Instruments, Brno, Czech Republic). The cells were irradiated with ∼50 μmol photons·mol^{-1}·cm^{-2} of light from red and white LEDs and aerated with compressed air. The cells were harvested at the late log phase, pelleted at 6000 g, and resuspended in Tris-Cl (50 mM, pH 9.5, at room temperature) with KCl (125 mM) (Buffer S) to yield 1 mg/mL chlorophyll (Chl *a*) solutions. The cells were then incubated at 40 °C in Buffer S with 0.0025% (w/v) lysozyme (Gold Bio, United States) for 1 h in the dark, at 250 rpm on an orbital shaker. The intact cells were then pelleted at ∼10,000 g for 10 min, resuspended in Buffer S, and Dounce-homogenized. The cells were then mechanically lysed (×10) using a benchtop LM10 microfluidizer (Microfluidics, Westwood, MA) at 23,000 psi. The intact cells and debris material were pelleted at ∼10,000 g for 10 min and discarded. The thylakoid membranes contained in the supernatant were then pelleted at ∼190,000 g. This pellet was resuspended using a brush and was Dounce-homogenized in Buffer S (×3) to remove membrane-associated proteins.[8] The resultant thylakoid membranes were then diluted to 1 mg/mL chlorophyll and stored at −20 °C prior to solubilization.

Membrane Solubilization and Protein Isolation Using SMALPs. Thylakoid membrane aliquots (500 μL) were incubated with an alkoxy-functionalized SMA copolymer in the dark at a final concentration of 1.5% (w/v) for 3 h at 40 °C, while shaking (250 rpm, orbital shaker). The samples were centrifuged at ∼190,000 g for

https://doi.org/10.1021/acs.biomac.1c00274
Biomacromolecules 2021, 22, 2544−2553

15 min, and the supernatant was removed using a flame-drawn Pasteur pipette. These supernatants, which contain PSI-SMALPs, were then analyzed directly or were further purified using sucrose density gradients and ultracentrifugation.

Sucrose Density Gradient Ultracentrifugation. The PSI-SMALP-containing supernatants were then purified by sucrose density gradient centrifugation (SDGC) using a linear gradient of 10−30% (w/v) on a 50% (w/v) sucrose cushion. Next, 1 mL of SMA-solubilized supernatant was loaded on the top of the gradient and centrifuged in a SW-32 swinging bucket rotor for 20 h at ∼150,000 g. The lowest green band was harvested using a needle syringe. This band has been shown to be PSI-SMALP.

Protein Analyses. Absorbance spectroscopy was performed using a dual-beam benchtop spectrophotometer (Evolution 300, Thermo Scientific). Following solubilization and high-speed sedimentation, the supernatants were diluted (×20) prior to absorbance measurements. Chlorophyll was extracted with 90% methanol at 65 °C for 2 min, as previously described,[13] and absorbance was taken at 665 nm to determine chlorophyll concentration.

Sodium dodecyl sulphate−polyacrylamide gel (SDS−PAGE) analysis was performed using a sample solubilization buffer containing ∼350 mM dithiothreitol and 4% SDS. The samples were heated in a 65 °C water bath for 9 min prior to loading onto a Bio-Rad TGX stain-free Criterion pre-cast gel. The gel was then illuminated and fixed prior to the imaging of the TGX fluorochrome using a Bio-Rad ChemiDoc MP gel imaging system.

Low temperature fluorescence was obtained at 77 K on presumed trimeric PSI bands following sucrose density gradient ultracentrifugation using the previously reported methods.[14] These analyses were performed using a PTI Quantamaster dual-channel fluorimeter (HORIBA, Kyoto, Japan). Spectra are averaged over three measurements following background subtraction and normalized to the maximum fluorescence.

Transmission Electron Microscopy. PSI-SMALPS were isolated using sucrose density gradient ultracentrifugation. The isolated SMALP samples were diluted (×10−50) into Buffer S. A copper-coated grid was placed in a 20 μL drop of the sample solution for 1 min. Excess sample was removed via filter paper absorption, and the grid was washed by dipping it in distilled water. Excess distilled water was removed via filter paper absorption. The grid was then immediately stained by placing it in a 20 μL drop of 1% uranyl acetate for 1 min. The grid was allowed to dry and imaged using a JEOL 1440-Flash TEM at 200 kV.

RESULTS AND DISCUSSION

Synthesis and Characterization of SMA Derivatives. In this study, PRO 10235 (**PRO**), a commercially available copolymer of styrene and maleic anhydride, was functionalized with various alkoxy ethoxylates by DMAP-catalyzed esterification to yield polymers **Eth-Dodec** (Scheme 1). Additionally, two control polymers were functionalized with either diethylene glycol or tetraethylene glycol moieties to produce polymers **DEG** and **TEG**, respectively, so as to probe the role that the hydrophobicity of alkoxy ethoxylates has on the extraction process. For each esterification reaction, aliquots were taken as a function of reaction time to obtain polymer samples with increasing amounts of the attached sidechains. These aliquots were purified by washing and dried in a vacuum oven to remove unreacted reagents and solvents. ^{1}H NMR spectroscopy was employed to determine the extent of esterification for each sample (Figures S3-S11). As a note, individual polymer identifiers will be used herein to identify a specific degree of esterification for each polymer sample. For example, polymer **Eth** with 16% monoesterified acid groups will be referred to as **Eth-(16)**.

Determination of pH Sensitivity. To determine how sidechain functionalization affects polymer solubility as a function of pH, each polymer was introduced to a series of BR-buffers ranging from pH = 4.5 to 10, in half unit increments. As pH becomes more acidic, the polymers studied convert from their carboxylate forms to their carboxylic acid forms, thereby becoming insoluble in aqueous media, and aggregation is observed. Thus, polymer aggregation can be quantified by measuring the increase in optical density at 350 nm (Figure 1a). Our results show that unmodified PRO 10235 remained soluble at all pH values tested, as was expected from the prior literature reports.[12] For SMA derivatives **Eth-Dodec**, their low pH tolerance decreased as a function of increasing percentage esterification. As expected, this effect is amplified when functionalized with more hydrophobic moieties (e.g., **Eth-Dodec**) as compared to more hydrophilic **DEG**/**TEG** substituted polymers, which remain soluble at lower pH values, even as the esterification percentage increased. All the solubility data as a function of pH can be found in the Supporting Information (Figure S14).

Scheme 1. Synthesis of Esterified SMA Derivatives

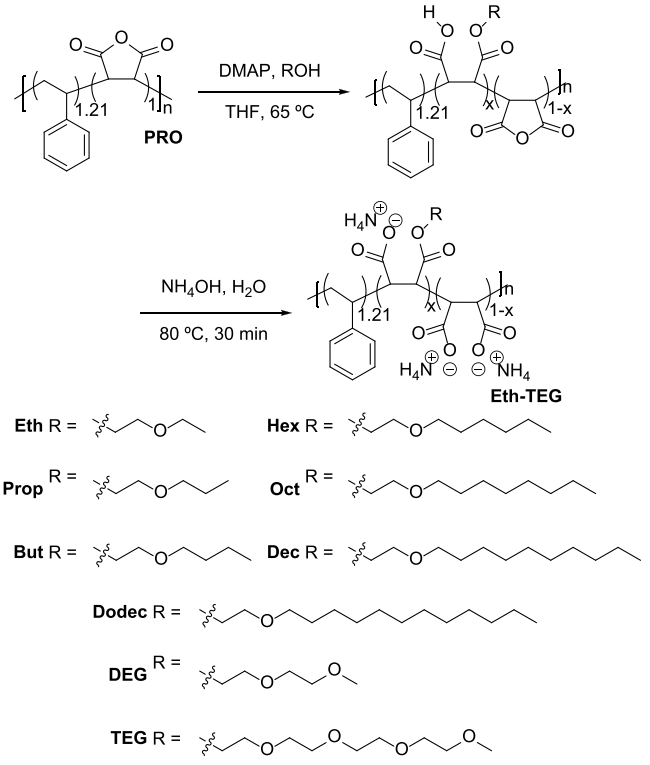

Determination of Divalent Cation Sensitivity. Another important characteristic is how well the synthesized SMA derivatives tolerate divalent cations. For this assay, each polymer was subjected to a series of pH = 9.5 tris buffers containing increasing concentrations of $MgCl_2$ (Figure 1b). Polymers **Eth-Dodec** were each found to be sensitive to divalent ions, with most beginning to aggregate in the presence of ≤10 mM $MgCl_2$. Furthermore, divalent ion sensitivity increases with increasing percentage esterification. In contrast, **DEG** and **TEG** polymer samples show a reverse trend, becoming more divalent ion-tolerant as the degree of esterification is increased, and with **TEG-(44)** and **TEG-(62)** remaining soluble at 100 mM $MgCl_2$, which is the highest concentration tested. These sidechains contain ethereal units that are known to complex cations and promote solubility in aqueous environments.[15] All solubility data as a function of

https://doi.org/10.1021/acs.biomac.1c00274
Biomacromolecules 2021, 22, 2544−2553

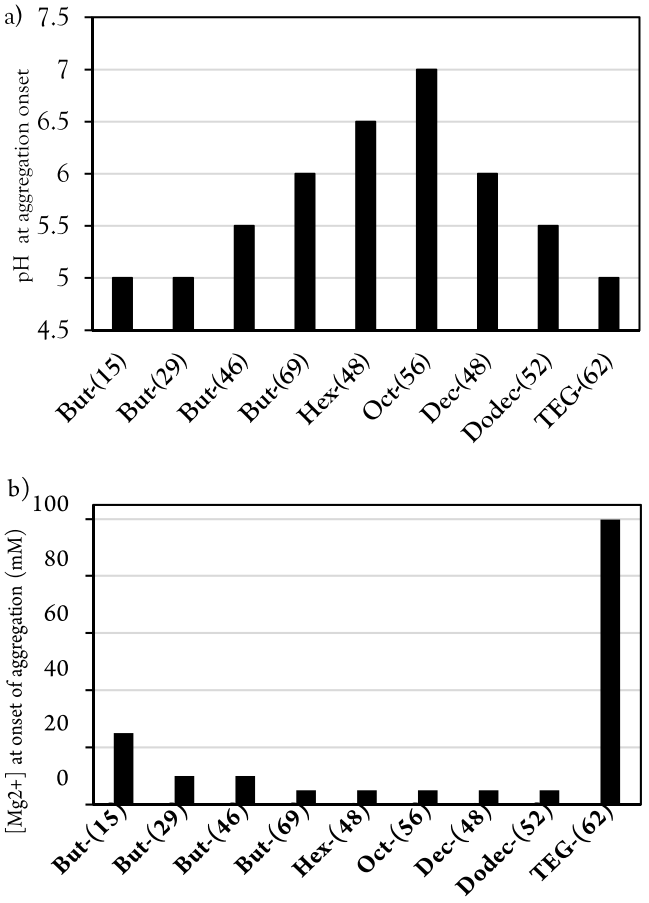

Figure 1. Bar graphs showing the (a) pH below which and (b) concentration of $MgCl_2$ above which each the polymer aggregates and precipitates from the solution. *TEG-(62) remained soluble at a concentration of 100 mM of Mg^{2+}.

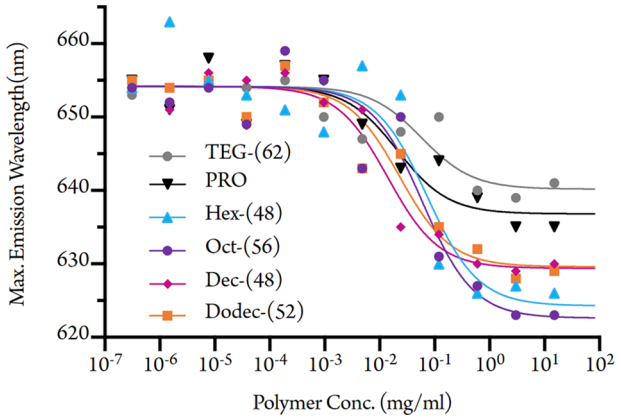

Figure 2. Plot of fluorescence emission wavelength maxima (see Figure S16) as a function of polymer concentration. Data were fit using a sigmoidal curve to represent each sample's CAC.

divalent cation concentration can be found in the Supporting Information (Figure S15).

Determination of CAC. To determine the polymer concentration at which aggregation occurs, which is often referred to as CAC, we employed a previously described method by fluorescence spectroscopy and Nile Red as a reporter.[12] Upon excitation at 550 nm, the fluorescence emission maximum of Nile Red blue shifts as it partitions into a hydrophobic environment. Therein, the extent of emission maximum blue shift corresponds to increased hydrophobicity in solution, which arises due to the aggregation of the polymers in the solution. The plots of fluorescence wavelength maxima as a function of concentration yield a sigmoidal relationship that reveals that aggregation for the highest percentage esterified SMA copolymers occurs in the range ~20−100 μg/mL, with the exception of **TEG-(62)** that aggregates around 0.6 to 3 mg/mL (Figure 2 and S16). Interestingly, we also observed that SMA derivatives functionalized with hydrophobic sidechains (**Hex-Dodec**) exhibited larger fluorescence maxima blueshifts than the more hydrophilic polymers **PRO** and **TEG-(62)** (Figure S17), agreeing with our hypothesis that the aggregation of **Hex-Dodec** will generate a more hydrophobic environment for Nile red partitioning.

Solubilization of Pigment−Protein Complexes from Te. To investigate the protein extraction efficiency and selectivity, each alkoxy-functionalized SMA copolymer derivative was incubated with isolated Te thylakoid membranes. This resulted in the solubilization of PSI, similar to our previous works.[8,14] Following centrifugation, the solubilized PSI complexes, which are pigmented with carotenoids and chlorophyll, remained in the supernatant while nonsolubilized material sedimented. The supernatant was then analyzed by visible absorbance spectroscopy to qualitatively determine the carotenoid and chlorophyll content. The peaks arising from carotenoids overlap in the spectral region between 425 and 550 nm, overlaying the Soret band for chlorophyll that is centered at 440 nm. Traces of phycocyanin (λ_{MAX} = ~625 nm) and a prominent chlorophyll absorbance peak at ~680 nm were also observed (Figure S18).[16]

The alkoxy ethoxylate-functionalized SMAs **Prop-Dodec** displayed an increasing qualitative trend of carotenoid release as a function of increasing percentage esterification, as evidenced by an increase in absorbance (Figure S18). A similar qualitative trend is observed with regard to the amount of chlorophyll being liberated (Figure S18). While these absorbance spectra are not fully quantitative, they enable us to make qualitative observations as to the effect that polymer functionalization has on their ability to liberate PSI, although while retaining the profiles of both carotenoids and chlorophyll within the complex. The increasing absorbances of both carotenoids and chlorophyll as a function of increasing polymer functionalization suggest that the amount of PSI extracted increases similarly and that these complexes retain their associated pigments following the removal from the thylakoid membrane.

Control polymer **DEG** displayed the opposite qualitative trend in the solubilization of chlorophyll-containing proteins, wherein higher percentages of esterification appear to decrease the amount of chlorophyll-containing proteins being liberated from the membrane. Furthermore, control polymer **TEG** showed no discernible solubilization trend at all (Figure S19a and S19b). Absorbance profiles for the supernatants of SMA 1440 and DDM were also measured as controls to ensure consistency across all trials. Lastly, the absorbance profile for the supernatant resulting from membrane extraction with DMAP showed very little absorbance between 400 and 800 nm (Figure S19c), suggesting that potential for trace amounts of this reagent remaining in the synthesized polymer samples did not artificially impact our results.

https://doi.org/10.1021/acs.biomac.1c00274
Biomacromolecules 2021, 22, 2544−2553

To quantify the percentage solubilization efficiency (SE) of extracted chlorophyll proteins of each SMA formulation, we compared extracted chlorophyll in the supernatant to the 1 mg/mL chlorophyll of the starting thylakoid membrane and reported this as a percentage (Figure 3). Quantification of this

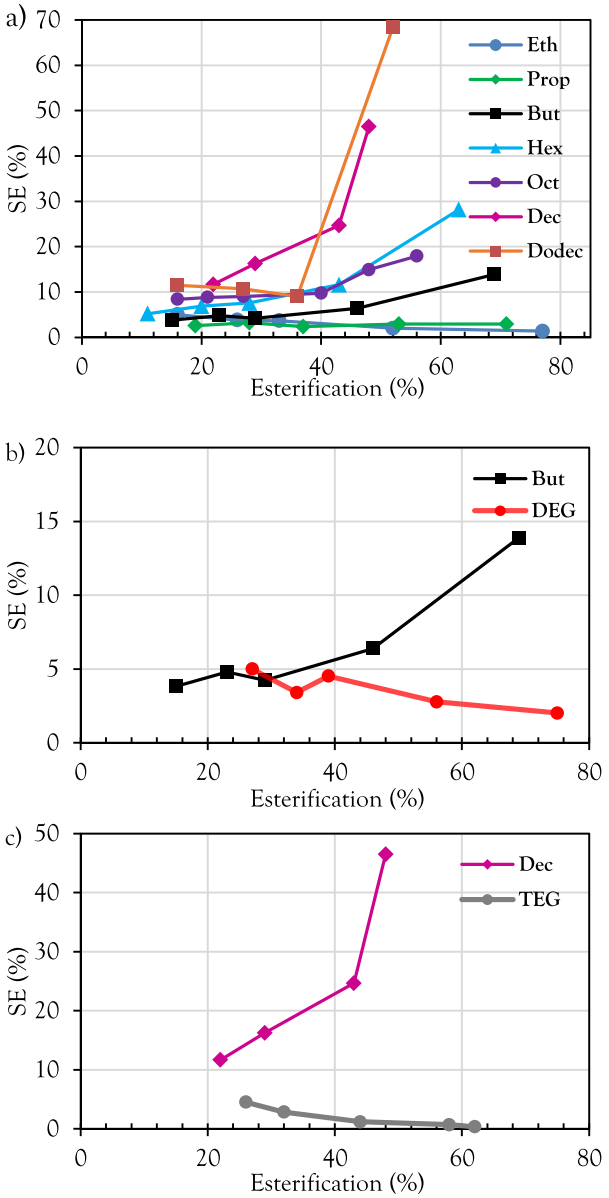

Figure 3. Comparison of the percentage SE of chlorophyll and chlorophyll-containing complexes as a function of percentage esterification for (a) SMA-based copolymers **Eth-Dodec** that are functionalized with alkoxy ethoxylate sidechains, (b) polymers **But** and **DEG** that each contain six atoms in their sidechains but that differ in the number of ether units present, and (c) polymer samples **Dec** and **TEG** that each contain thirteen atom sidechains but that differ in the number of ether units present.

data confirms what was qualitatively observed: the longer alkoxy ethoxylate sidechains tend to elicit a higher solubilization efficiency than shorter alkoxy ethoxylates, especially as percentage esterification increases. Furthermore, these trends suggest that the sidechain length alone is not the primary factor, resulting in the increased SE. Rather, the increased hydrophobicity of the sidechain appears to have the most notable impact. This can be seen by comparing the alkoxy ethoxylate sidechains to the ethylene glycol sidechains of similar lengths (Figure 3b,c). For instance, polymers **But** and **DEG** both have six-atom sidechains. However, **DEG** is much more hydrophilic because of the additional ethereal units present. The same observation holds true for polymers **Dec** and **TEG**, both containing sidechains thirteen atoms long, although **TEG** is more hydrophilic because of the attached tetraethylene glycol moiety. In both instances, the more hydrophilic polymer exhibits a markedly higher percentage SE in the extraction of PSI from Te, particularly at high degrees of esterification.

Although the trends shown in Figure 3 are informative, it is difficult to draw direct comparisons relating hydrophobicity and the SE when the polymers studied bear varying extents of esterification as well as different length alkoxy moieties. As such, a simple method to normalize the relative hydrophobicity of polymers **Eth-Dodec** was needed. To accomplish this, we chose to compare these polymers based upon their number of side-chain carbons per the average number of carboxylate moieties present in the polymeric repeat unit. Therein, the average number of carboxylates per repeat unit was calculated based upon (a) percentage esterification and (b) knowing that unfunctionalized maleic acid units contain two carboxylates, whereas monoesterified maleic acid units contain only one carboxylate. The number of carbons per alkoxylated ester (e.g., decyloxyethoxy units contain 14 carbons) was then divided by the average number of carboxylates per repeat unit to obtain a new metric that relates the hydrophobic sidechain content to the hydrophilic carboxylate content. SE was then plotted as a function of the average number of carboxylates per maleic acid (Figure 4).

The data in Figure 4 indicate that both longer alkoxy ethoxylates and higher extents of esterification lead to higher SEs. As an example, although **Oct-(56)-** and **Dodec-(52)-**bearing octyloxy and dodecyloxy substituents, respectively, have very similar degrees of esterification, the latter features a SE that is ∼400% higher than that of the former. We hypothesize that this is indicative of increased interactions between longer alkoxy ethoxylate sidechains and the tails of the galactolipids present in the thylakoid membrane of Te. Unfortunately, attaching longer alkoxy chains to **PRO** also leads to a large decrease in the aqueous solubility. This became problematic for polymers **Oct**, **Dec**, and **Dodec** that gelate in water when functionalized beyond ∼55% esterification, as attempts to solubilize membrane proteins require water-soluble polymers. This suggests that although increasing the chain length and the degree of esterification appears to favor higher SEs, polymer samples functionalized with hydrophobic sidechains will eventually become too hydrophobic to remain in the solution.

Another striking feature observed in Figure 4 is that an empirical threshold of esterification was observed at ∼50%, beyond which a drastic increase in the percentage SE is observed for polymers **Hex**, **Dec**, and **Dodec.** This effect is amplified as the length of the attached alkoxy ethoxylate increases, as illustrated by comparing the polymer samples functionalized at both low and high degrees of esterification (Figure 5). When comparing samples featuring ∼30% esterification of different alkoxy sidechains, the samples with longer sidechains exhibit a slightly higher SE (Figure 5a). In contrast, SE increases significantly between the samples as the degree of esterification is pushed past the empirical threshold

https://doi.org/10.1021/acs.biomac.1c00274
Biomacromolecules 2021, 22, 2544−2553

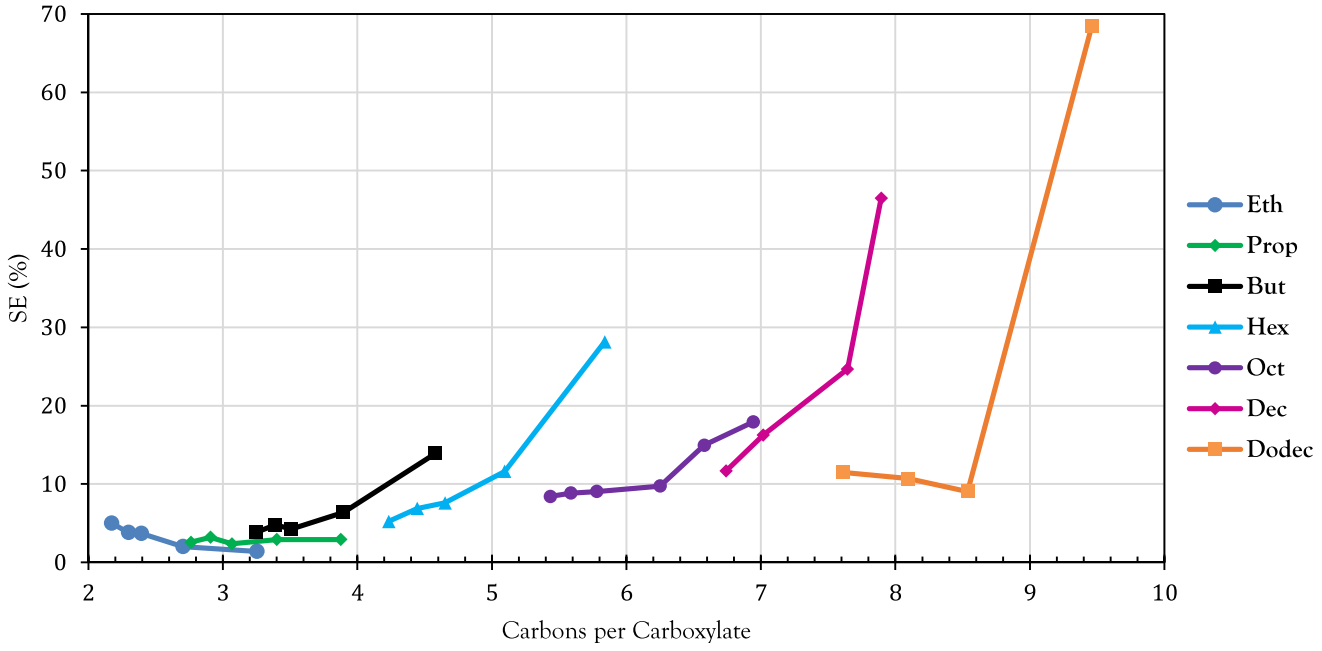

Figure 4. Percentage SE as a function of sidechain carbons per carboxylate as a metric reflecting the relative hydrophobicity of polymers **Eth-Dodec**.

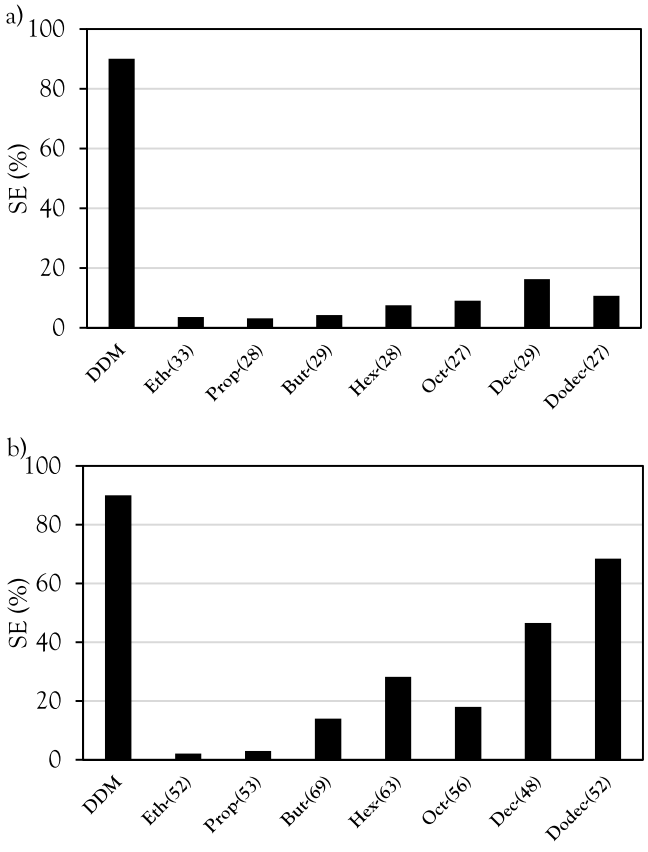

Figure 5. Percentage SE of esterified SMA copolymers at (a) low degrees of esterification and (b) high degrees of esterification, and measured as percentage chlorophyll in the supernatant, following thylakoid membrane solubilization and high-speed sedimentation.

of 50% esterification. For example, while the dodecyloxy-substituted **Dodec-(27)** elicits an 41% increase in SE compared to the hexyloxy-substituted **Hex-(28)**, **Dodec-(52)** achieves a SE 143% higher than **Hex-(63)** (Figure 5b).

Characterization of Pigment–Protein Complexes Isolated from Te. To determine whether the chlorophyll extracted using the SMA derivatives reported herein is bound to protein complexes or free in solution, the supernatant following membrane solubilization was purified using a sucrose density gradient (Figure 6). As can be seen in Figure 6, the top

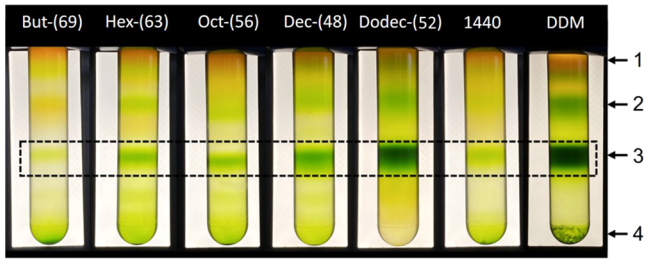

Figure 6. Sucrose density gradients of PSI-SMALPs following solubilization with alkoxy-functionalized SMA copolymers. The black dashed box indicates the trimeric PSI band. Numbers to the right indicate the band number discussed in the text.

orange band contains free carotenoids (band 1). Further down the gradient is a diffuse green band containing free chlorophyll, and, in the case of DDM, monomeric PSI and PSII (band 2).[17] The trimeric PSI band is highlighted in the black, dashed box (band 3), and larger PSI particles (aggregates in the case of DDM) can be seen at the bottom of the gradient (band 4). Interestingly, the samples with longer alkoxy ethoxylates resulted in the formation of more SMALPs containing single PSI trimers, rather than larger, high-density chlorophyll-containing fractions. We previously reported that these larger sections of the high-density thylakoid membrane are found near the bottom of the sucrose gradient and contain PSI (presumably in the trimeric form).[8] In the case of polymer

https://doi.org/10.1021/acs.biomac.1c00274
Biomacromolecules 2021, 22, 2544−2553

Dodec, the larger chlorophyll-containing complexes are completely absent.

It should also be noted that some aggregated chlorophyll-containing protein complexes can be seen on the 50% sucrose (w/v) cushion at the bottom of the DDM gradient, as additional DDM was not included in this sucrose gradient buffer to maintain the dynamic equilibrium between DDM micelles and DDM bound to the PSI toroid. However, for the purposes of this control, trimeric PSI is shown to be the dominant species arising from DDM isolation. Therefore, we consider this control to be acceptable. Lastly, this side-by-side comparison allows us to observe that the SMALPs do not seem to require excess SMA in solution to maintain the integrity of the formed nanodiscs.

The trimeric PSI containing band 3 was harvested from each sucrose density gradient and was imaged using transmission electron microscopy (TEM) and a negative stain, with the exception of **But-(69)** because of low yield, to provide evidence of derivatized SMALP formation. A representative micrograph of **Dodec-(52)** is shown in Figure 7 (others are shown in Figure S20), which provides clear evidence of derivatized SMALP formation. The average diameter of the SMALPs (n = 10) are listed in Table 1, wherein **Oct-(59)** was found to form the largest discs, followed by **Hex-(53)**, **Dodec-(52)**, and **Dec-(60)**. Interestingly, this pattern seems to correlate with the pH stability study and the maximum blue shifts recorded, as shown in Figure S16. These data may suggest that optimum hydrophobicity may be achieved using SMA derivative **Oct-(59)**, which allows this copolymer to stabilize larger lipid annuli around the trimeric PSI-SMALPs, while at the same time narrowing the solubility conditions of the polymer itself.

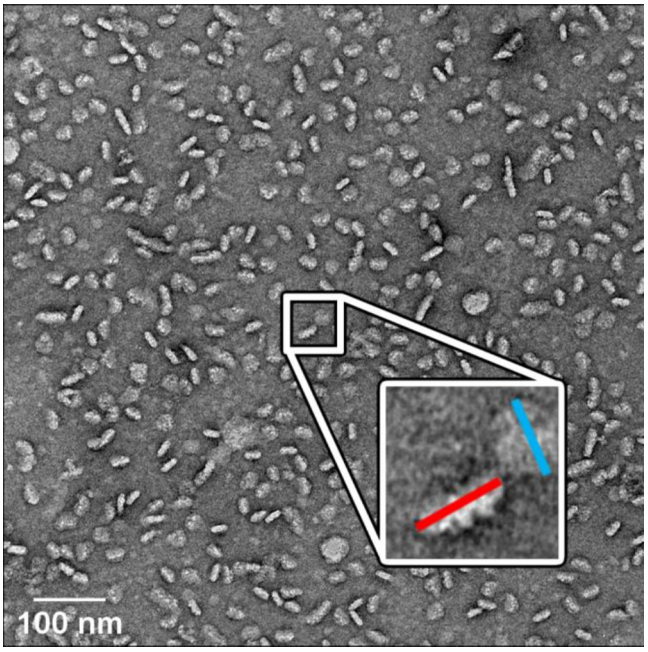

Figure 7. TEM of derivatized SMALPs formed by the solubilization of PSI from Te using **Dodec-(52)**. The red and blue bars depicted in the micrograph inset represent distances measured to determine average diameters, wherein the blue bar depicts measurement across the face of a SMALP, and the red bar represents measurement along the side of a SMALP.

Table 1. Average Measured Diameters of Derivatized PSI-SMALPs[a]

solubilizing agent	avg. diameter (nm)	standard deviation (nm)	standard error (nm)
DDM	21.5	2.5	0.8
1440	34.7	5.4	1.7
Hex-(53)	31.2	4.3	1.4
Oct-(59)	35.4	6.1	1.9
Dec-(60)	26.8	2.2	0.7
Dodec-(52)	28.4	6.8	2.2

[a]Deviation and error are calculated based upon the measurement of 10 SMALPs using the ImageJ software.

The trimeric PSI fractions were collected and separated using SDS−PAGE to determine their polypeptide profiles (Figure 8). As we hypothesized, the typical PSI profile was observed across all SMA copolymers tested. Interestingly, the peripherally associated PsaF subunit seems to be missing in the SMA 1440 control but not in the alkoxy-functionalized SMAs synthesized herein or DDM. We have previously reported that PsaF can be lost over time in PSI-SMALPs formed with the commercially synthesized SMA 1440 copolymer.[8] It was posited in this work that the hydrophobic interaction between the peripheral subunit PsaF and the outer edge of the PsaB core subunit, facilitated by a carotenoid molecule, may create a dynamic equilibrium in vivo between a PsaF bound state and a pool of free and unbound PsaF that has been previously reported in cyanobacterial thylakoids.[18] While this may also be the case observed here, our results suggest that PsaF may not be lost simply because of the ability to dissociate from the core complex within the confines of the lipid annulus, but rather, the disruption of this PsaF to PsaB interaction may be more complicated and require further investigations.

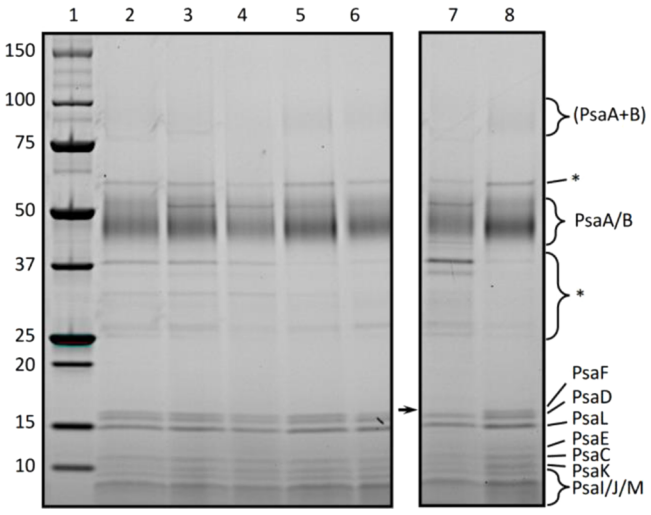

Figure 8. SDS−PAGE of PSI-SMALP trimer bands following solubilization with various alkoxy-functionalized SMA copolymers. Shown here are **Hex-(63)** (lane 1), **Oct-(48)** (lane 2), **Dec-(43)** (lane 3), **Dec-(48)** (lane 4), **Dodec-(52)** (lane 5), MW standard (lane 6), SMA 1440 (lane 7), and DDM (lane 8). Subunits are labeled in the right side. Regions marked with an asterisk contain unknown contaminants, (PsaA+B) denotes the undissociated heterodimer, whereas PsaA/B represents their respective monomers, and the black arrow denotes the missing PsaF band in lane 7.

https://doi.org/10.1021/acs.biomac.1c00274
Biomacromolecules 2021, 22, 2544−2553

Low-temperature fluorescence emission scans at 77 K of the presumed PSI trimer-containing fractions were performed to further confirm the formation of PSI-containing SMALPs (Figure 9). Following excitation at 430 nm, free chlorophyll in

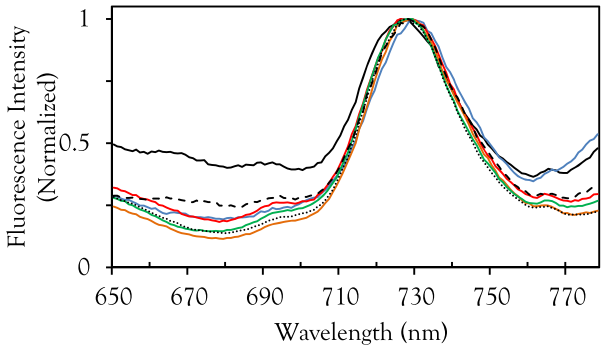

Figure 9. Normalized chlorophyll fluorescence emission spectra for trimeric PSI containing SMALPs isolated using alkoxy ethoxylate-functionalized SMA copolymers following sucrose density gradient ultracentrifugation. Shown here are **But-(69)** (black, solid line), **Hex-(63)** (blue), **Oct-(48)** (red), **Dec-(48)** (orange), **Dodec-(52)** (green), SMA 1440 (black, dashed line), and DDM (black, dotted line).

the solution exhibited fluorescence at <680 nm, as well as a very minor peak at 695 nm signifying minimal extraction of PSII.[19] The bulk of the fluorescence signal stems from chlorophyll bound to PSI with a characteristic F_{MAX} red-shifted to ~730 nm. All functionalized PSI-SMALPs showed very little free chlorophyll/PSII and display an F_{MAX} of 728–729 nm, with the exceptions of **But-** and **Oct-**functionalized SMALPs (Figure S18). In the case of polymer **But**, this may be due to the low concentration of PSI-SMALP in the sample, decreasing the signal of the characteristically red-shifted absorbance of chlorophyll in Te PSI, therefore resulting in a blueshift in the fluorescence emission maximum. For polymer **Oct**, we suspect that this observation is due to an aberrant spike in one triplicate scan, artificially skewing the average F_{MAX} for this triplicate average. However, the peak centers around 729 nm.

CONCLUSIONS

Little is known about how altering the chemical composition of SMAs and SMA derivatives affects the efficiency and selectivity of membrane protein extraction. Herein, we report evidence that alkoxy ethoxylate esterified SMAs can be used to promote the solubilization of trimeric PSI from Te via the formation of derivatized SMALPs. We observed that increasing the relative hydrophobicity of the amphiphilic copolymer leads to an overall increase in the amount of trimeric PSI extracted from the cyanobacterium Te membranes. From these results, two main characteristics of functionalized SMA copolymers were identified to have large impacts on protein extraction. First, SMA derivatives bearing longer alkoxy ethoxylate sidechains, such as dodecyloxy-substituted **Dodec**, tend to elicit higher SEs as compared to polymers bearing shorter alkoxy ethoxylate sidechains; however, our data also suggest that the length of the sidechain is not the only factor to be considered. Second, the number of attached sidechains appears to be an even more important factor with regard to efficient protein solubilization. To highlight this feature, we observed a drastic increase in the SE as the extent of polymer monoesterification surpassed 50%, an effect which is more apparent when studying longer alkoxy ethoxylate sidechains.

These two discoveries provide fundamental insights into the mechanism of SMA-facilitated protein solubilization in Te. We hypothesize that the aliphatic chains aid in SMALP formation by anchoring into the acyl chain region of the membrane, similar to the action of the styrene moiety of SMAs utilized in previous studies.[20] Other groups have noted the possibility of amphiphilic polymers utilizing functionalized sidechains to intercalate within the acyl chains present in the tails of membrane lipids.[21] We suspect that our alkoxy ethoxylates are functioning in a similar manner, wherein longer alkyl chains can more effectively anchor because of favorable interactions with the tails of the galactolipids composing the membrane. Finally, we hypothesize that polymers featuring higher degrees of esterification may drive preferential insertion into the lipid bilayer and initiate SMALP formation. This could explain the steep increase in solubilization observed when esterification percentages surpass the empirically observed 50% esterification threshold. This suggests a critical equilibrium between the aqueous solubility of the modified polymers and the increased partitioning into the lipid bilayer; further work will be needed to see how this process is affected by fatty-acid composition, lipid headgroup composition, and temperature.

ASSOCIATED CONTENT

Supporting Information

The Supporting Information is available free of charge at https://pubs.acs.org/doi/10.1021/acs.biomac.1c00274.

NMR characterization of the functionalized SMA copolymers; GPC characterization of PRO 10235; absorbance spectra of negative controls; all data of the SE as a function of percentage functionalization; pH tolerance of SMA derivatives; cation tolerance of SMA derivatives; and TEM images of isolated SMALPs (PDF)

AUTHOR INFORMATION

Corresponding Authors

Barry D. Bruce − *Department of Biochemistry & Cellular and Molecular Biology, University of Tennessee, Knoxville 37996-1939, Tennessee, United States; Department of Chemical and Biomolecular Engineering, University of Tennessee, Knoxville 37996-0840, Tennessee, United States;* orcid.org/0000-0002-4045-9815; Email: bbruce@utk.edu

Brian K. Long − *Department of Chemistry, University of Tennessee, Knoxville 37996-1600, Tennessee, United States;* orcid.org/0000-0002-2691-6194; Email: long@utk.edu

Authors

Nathan G. Brady − *Department of Biochemistry & Cellular and Molecular Biology, University of Tennessee, Knoxville 37996-1939, Tennessee, United States;* orcid.org/0000-0002-3443-8006

Cameron E. Workman − *Department of Chemistry, University of Tennessee, Knoxville 37996-1600, Tennessee, United States*

Bridgie Cawthon − *Department of Chemical and Biomolecular Engineering, University of Tennessee, Knoxville 37996-0840, Tennessee, United States*

Complete contact information is available at: https://pubs.acs.org/10.1021/acs.biomac.1c00274

https://doi.org/10.1021/acs.biomac.1c00274
Biomacromolecules 2021, 22, 2544−2553

Author Contributions

[‖]N.G.B. and C.E.W. contributed equally.

Funding

Support for BDB has been provided from the Gibson Family Foundation, the Dr. Donald L. Akers Faculty Enrichment Fellowship, and the National Science Foundation (EPS-1004083). NGB and BDB have been supported via a Joint Directed Research Development Award from the University of Tennessee at Knoxville/Oak Ridge National Laboratory Science Alliance. NGB has also been supported via a Penley Fellowship, James and Dora Wright Fellowship, and a UTK Graduate School Fellowship. BKL and CEW were supported by the University of Tennessee's Office of Research and Engagement Seed Funding Program. BC was supported by UTK's Student Mentoring and Research Training Program. The JEM 1400 high-contrast TEM used in this work was purchased via an NSF MRI (MRI-1828300) to BDB and BKL.

Notes

The authors declare no competing financial interest.

■ ACKNOWLEDGMENTS

We would like to acknowledge Mr. Joytirmoy Mondal and Ms. Katrina Micin for maintaining the cyanobacteria and growing the 125-liter cultures of *T. elongatus*. The PRO 10235 powder was a generous gift from Mr. Ryan Beer at TOTAL Petrochemicals USA. We thank Dr. Olena Korotych for insightful discussions prior to the beginning of htis work. We would like to thank Dr. Jaydeep Kolape for his assistance and guidance with TEM. We would also like to thank Dr. Michael Best for his fruitful insights into this project.

■ ABBREVIATIONS

Chl chlorophyll
PSI photosystem I
SE solubilization efficiency
SMA styrene−maleic acid copolymer
SMALP styrene−maleic acid lipid particle
S:MA styrene:maleic acid ratio
Te *Thermosysnechococcus elongatus*
SDS−PAGE sodium dodecyl sulfate−polyacrylamide gel electrophoresis
GPC gel permeation chromatography
NMR nuclear magnetic resonance
DOSY diffusion-ordered spectroscopy.

■ REFERENCES

(1) Dörr, J. M.; Koorengevel, M. C.; Schäfer, M.; Prokofyev, A. V.; Scheidelaar, S.; van der Cruijsen, E. A. W.; Dafforn, T. R.; Baldus, M.; Killian, J. A. Detergent-free isolation, characterization, and functional reconstitution of a tetrameric K+ channel: The power of native nanodiscs. *Proc. Natl. Acad. Sci. U. S. A.* **2014**, *111*, No. 18607.

(2) Domínguez Pardo, J. J.; Koorengevel, M. C.; Uwugiaren, N.; Weijers, J.; Kopf, A. H.; Jahn, H.; van Walree, C. A.; van Steenbergen, M. J.; Killian, J. A. Membrane Solubilization by Styrene−maleic acid Copolymers: Delineating the Role of Polymer Length. *Biophys. J.* **2018**, *115*, 129−138.

(3) Morrison, K. A.; Akram, A.; Mathews, A.; Khan, Z. A.; Patel, J. H.; Zhou, C.; Hardy, D. J.; Moore-Kelly, C.; Patel, R.; Odiba, V.; Knowles, T. J.; Javed, M.-U.-H.; Chmel, N. P.; Dafforn, T. R.; Rothnie, A. J. Membrane protein extraction and purification using styrene−maleic acid (SMA) copolymer: effect of variations in polymer structure. *Biochem. J.* **2016**, *473*, 4349.

(4) Ravula, T.; Hardin, N. Z.; Ramadugu, S. K.; Ramamoorthy, A. pH Tunable and Divalent Metal Ion Tolerant Polymer Lipid Nanodiscs. *Langmuir* **2017**, *33*, 10655−10662.

(5) Burridge, K. M.; Harding, B. D.; Sahu, I. D.; Kearns, M. M.; Stowe, R. B.; Dolan, M. T.; Edelmann, R. E.; Dabney-Smith, C.; Page, R. C.; Konkolewicz, D.; Lorigan, G. A. Simple Derivatization of RAFT-Synthesized Styrene−Maleic Anhydride Copolymers for Lipid Disk Formulations. *Biomacromolecules* **2020**, *21*, 1274−1284.

(6) Esmaili, M.; Acevedo-Morantes, C.; Wille, H.; Overduin, M. The effect of hydrophobic alkyl sidechains on size and solution behaviors of nanodiscs formed by alternating styrene maleamic copolymer. *Biochim. Biophys. Acta, Biomembr.* **2020**, *1862*, No. 183360.

(7) Korotych, O. I.; Nguyen, T. T.; Reagan, B. C.; Burch-Smith, T. M.; Bruce, B. D. Poly(styrene-co-maleic acid)-mediated isolation of supramolecular membrane protein complexes from plant thylakoids. *Biochim. Biophys. Acta, Bioenerg.* **2021**, *1862*, No. 148347.

(8) Brady, N. G.; Li, M.; Ma, Y.; Gumbart, J. C.; Bruce, B. D. Non-detergent isolation of a cyanobacterial photosystem I using styrene maleic acid alternating copolymers. *RSC Adv.* **2019**, *9*, 31781−31796.

(9) Phan, M. D.; Korotych, O. I.; Brady, N. G.; Davis, M. M.; Satija, S. K.; Ankner, J. F.; Bruce, B. D. X-ray and Neutron Reflectivity Studies of Styrene−maleic acid Copolymer Interactions with Galactolipid-Containing Monolayers. *Langmuir* **2020**, *36*, 3970−3980.

(10) Kharlamov, A. V.; Artyushin, O. I.; Bondarenko, N. A. Synthesis of some acyclic quaternary ammonium compounds. Alkylation of secondary and tertiary amines in a two-phase system. *Russ. Chem. Bull.* **2014**, *63*, 2445−2454.

(11) Francisco Martinez, G. N.; Torres, M. Monoesterification of Styrene-Maleic Anhydride Copolymers with Aliphatic Alcohols. *Bol. Soc. Chil. Quim.* **2001**, *46*, 137−141.

(12) Scheidelaar, S.; Koorengevel, M. C.; van Walree, C. A.; Dominguez, J. J.; Dörr, J. M.; Killian, J. A. Effect of Polymer Composition and pH on Membrane Solubilization by Styrene−maleic acid Copolymers. *Biophys. J.* **2016**, *111*, 1974−1986.

(13) Iwamura, T.; Nagai, H.; Ichimura, S.-E. Improved Methods for Determining Contents of Chlorophyll, Protein, Ribonucleic Acid, and Deoxyribonucleic Acid in Planktonic Populations. *Int. Rev. Gesamten Hydrobiol. Hydrogr.* **1970**, *55*, 131−147.

(14) Cherepanov, D. A.; Brady, N. G.; Shelaev, I. V.; Nguyen, J.; Gostev, F. E.; Mamedov, M. D.; Nadtochenko, V. A.; Bruce, B. D. PSI-SMALP, a Detergent-free Cyanobacterial Photosystem I, Reveals Faster Femtosecond Photochemistry. *Biophys. J.* **2020**, *118*, 337−351.

(15) Gokel, G. W.; Leevy, W. M.; Weber, M. E. Crown Ethers: Sensors for Ions and Molecular Scaffolds for Materials and Biological Models. *Chem. Rev.* **2004**, *104*, 2723−2750.

(16) Kennis, J. T. M.; Gobets, B.; van Stokkum, I. H. M.; Dekker, J. P.; van Grondelle, R.; Fleming, G. R. Light Harvesting by Chlorophylls and Carotenoids in the Photosystem I Core Complex of Synechococcus elongatus: A Fluorescence Upconversion Study. *J. Phys. Chem. B.* **2001**, *105*, 4485−4494.

(17) Rögner, M.; Nixon, P. J.; Diner, B. A. Purification and characterization of photosystem I and photosystem II core complexes from wild-type and phycocyanin-deficient strains of the cyanobacterium Synechocystis PCC 6803. *J. Biol. Chem.* **1990**, *265*, 6189−6196.

(18) Dühring, U.; Ossenbühl, F.; Wilde, A. Late assembly steps and dynamics of the cyanobacterial photosystem I. *J. Biol. Chem.* **2007**, *282*, 10915−10921.

(19) Lamb, J. J.; Rokke, G.; Hohmann-Marriott, M. F. Chlorophyll fluorescence emission spectroscopy of oxygenic organisms at 77 K. *Photosynthetica* **2018**, *56*, 105−124.

(20) Jamshad, M.; Grimard, V.; Idini, I.; Knowles, T. J.; Dowle, M. R.; Schofield, N.; Sridhar, P.; Lin, Y.; Finka, R.; Wheatley, M. Structural analysis of a nanoparticle containing a lipid bilayer used for detergent-free extraction of membrane proteins. *Nano Res.* **2015**, *8*, 774−789.

(21) Ball, L. E.; Riley, L. J.; Hadasha, W.; Pfukwa, R.; Smith, C. J. I.; Dafforn, T. R.; Klumperman, B. Influence of DIBMA Polymer Length

https://doi.org/10.1021/acs.biomac.1c00274
Biomacromolecules 2021, 22, 2544−2553

on Lipid Nanodisc Formation and Membrane Protein Extraction. *Biomacromolecules* **2021**, *22*, 763−772.

https://doi.org/10.1021/acs.biomac.1c00274
Biomacromolecules 2021, 22, 2544−2553